JOURNAL OF OPTOELECTRONICS AND ADVANCED MATERIALS, Vol. 11, No. 6, June 2009, p. 826 - 830

Titanium oxide thin films produced by pulsed laser deposition

C. SIMA*, C. GRIGORIU, C. VIESPE, I. PASUK[a], E. MATEI[a]
National Institute for Laser, Plasma and Radiation Physics, P.O. Box MG-36, Bucharest- Magurele, Romania.
[a] *National Institute of Materials Physics, P.O. Box MG-7, Bucharest-Magurele, Ilfov, 077125, Romania.*

The structural peculiarities of titanium oxide films formed by pulsed laser deposition have been investigated. A pure titanium target was irradiated by a Nd:YAG laser (355 and 532 nm). The work studied the influence of the beam wavelength, and oxygen pressure (20, 40, 80, and 160 mTorr) upon the layer structure. The films deposited at room temperature were partly crystalline. The crystalline fraction was a mixture of titanium sub-oxides. The 532 nm wavelength seems to favour the oxidation of titanium leading to TiO_2 formation even at room temperature. After annealing, crystalline TiO_2- anatase formed at both irradiation wavelengths, but only at low oxygen pressures (20 and 40 mTorr). The best crystallization occurs in the layers deposited at the lowest oxygen pressure (20 mTorr), at both laser beam wavelengths; most anatase formed in the sample obtained at 20 mTorr, 532 nm. At 20 mTorr the films were compact, for both wavelengths, but also tilted or randomly distributed columnar grains were observed at higher pressure. The films deposited with 355 nm, were thinner than those with 532 nm; at 355 nm the thickness decreased at higher pressure, while at 532 nm the dependence was opposite.

(Received December 15, 2008; after revision June 9, 2009; accepted June 15, 2009)

Keywords: Thin film, Pulsed laser deposition, Titanium oxides, Titanium sub-oxides structure, PLD

1. Introduction

Thin films of TiO_2 have attracted considerable interest in recent years, with widespread applications in several fields. They have high utility in solar energy conversion, photocatalysis, and gas sensors. Titanium oxide films can be obtained by numerous methods including pulsed laser ablation [1–18], magnetron sputtering [19, 20], electron beam evaporation [21], matrix-assisted pulsed laser evaporation [22, 23] and atomic layer deposition [24].

The formation of TiO_2 is known that depends on the deposition conditions, particularly the substrate temperature and the oxygen pressure [21].

In this study, titanium oxide thin films were deposited by pulsed laser deposition (PLD) from a titanium target in oxygen atmosphere, at room temperature. After deposition, the films were annealed at 350 ^{0}C.

The deposition was carried out at two laser wavelengths and four different oxygen pressures. The films were analysed by X-ray diffraction (XRD) and scanning electron microscopy (SEM).

2. Experimental

Titanium oxide thin films were deposited on optical glass at room temperature using an advanced computer-assisted PLD method, which allowed uniform irradiation of the entire target surface, taking into account the velocity and direction of the target movement, the laser pulse rate, the shape and size of the laser spot. A pure titanium target (99.99%) was irradiated using a Nd:YAG laser with a 10 pps repetition rate and 5-ns pulse duration. The deposition time was 4 hours for each film. The deposition was performed using two different laser beam wavelengths: 355 and 532 nm. The laser fluence was 3 J/cm^2 with 35 mJ energy/pulse. The substrate was placed at 4.5 cm from the target. The deposition chamber was evacuated to 1.6×10^{-5} Torr; the oxygen was maintained at a constant pressure of 20, 40, 80, and 160 mTorr. After deposition, the films were annealed at 350 ^{0}C for 2 hours in oxygen atmosphere. The structure of the films was analyzed by using a Bruker-AXS D8 ADVANCE X-ray diffractometer, in parallel beam setting, using $Cu_{K\alpha 1}$ monochromatized incident radiation. In order to enhance the signal coming from the film, the patterns were recorded in grazing incidence geometry, at an angle of 2^o. The scattered intensity was scanned between $5 \div 65^o$ (2θ). A simple attenuation calculus gives that in this geometry, the attenuation of the X-ray beam in 1500 nm thick TiO_2 film, measured at $2\theta = 20^o$ is around 90% (assuming a rough film density of 3.5 g/cm^3, which represents about 60% of the theoretical density of TiO and about 90% of that of anatase). This means that, almost the whole detected intensity results from the film and the signal coming from the substrate is almost completely attenuated.

The morphology of the film's surface and in the cross section was investigated by scanning electron microscopy (SEM) using a ZEISS EVO 60 microscope. Also, the film's thickness was estimated from the cross-sectional SEM images.

3. Results and discussion

The XRD patterns of the films deposited at RT obtained using 355 nm and 532 nm wavelengths, at different oxygen pressures, are presented in figure 1 and 2. The characteristic peaks of TiO, Ti_2O and Ti_3O were identified, superimposed on an intense amorphous background. The intensities are weak, and there are many superimposed lines. The identifications are based on the following reasons: the presence of TiO and Ti_3O is based on a single line at $2\theta=43.0^o$ and 37.6^o, respectively, while the Ti_2O presence is justified by the increased relative intensity of the TiO line at 37.1, where it superimposes on a Ti_2O line. All these phases appear in each film structure, in different concentrations, although sometimes the amount might be below the sensitivity limit of the graphical representations.

The examination of these figures shows that the formation of crystalline titanium oxide phases is clearly affected by the oxygen pressure in the deposition chamber, and depends also on the laser beam wavelength. As the pressure increases from 20 mTorr to 160 mTorr, the concentration of the titanium sub-oxides with smaller oxygen content (Ti_3O and Ti_2O) decreases while the structures enrich in TiO, regardless the laser beam wavelength. Comparing figure 1 and 2, one can observe that at the same oxygen pressure the concentration of titanium oxides with more oxygen is higher at λ=532 nm than at λ=355 nm. Therefore, it can be concluded that the oxidation of titanium is favoured using 532 nm wavelength. Only one of the as-deposited samples, obtained at 532 nm wavelength and at the highest oxygen pressure (160 mTorr) shows the characteristic diffraction lines of TiO_2, both anatase and rutile.

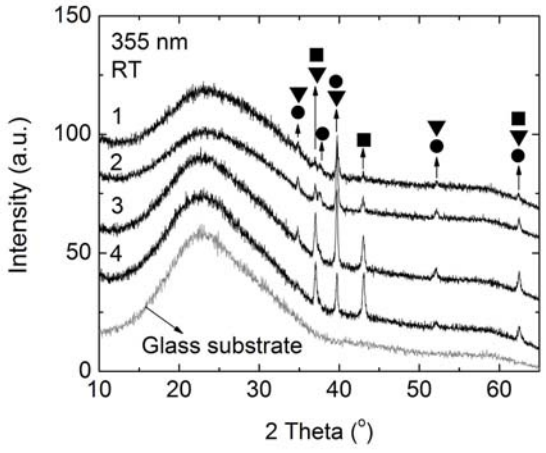

Fig. 1. XRD patterns of the films deposited at 355 nm, RT. Samples: 1 - 20 mTorr, 2 - 40 mTorr, 3 - 80 mTorr, 4 – 160 mTorr. Phases: ■ - TiO, ▼ - Ti_2O, ● - Ti_3O.

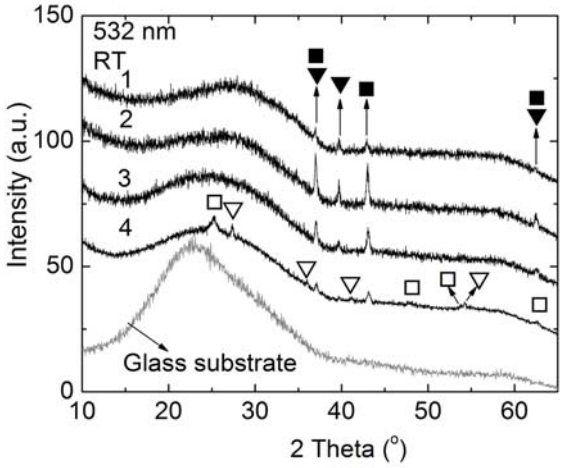

Fig. 2. XRD patterns of the films deposited at 532 nm, RT. Samples: 1 - 20 mTorr, 2 - 40 mTorr, 3 - 80 mTorr, 4 – 160 mTorr. Phases: ■ - TiO, ▼ - Ti_2O, □ - TiO_2 anatase, ▽ - TiO_2 rutile.

Based on the thicknesses measurements by SEM and taking into account the results of the above mentioned attenuation calculus, one can conclude that the films obtained at 532 nm are thicker than the penetration depth of X-rays, while those obtained at 355 nm are close to the penetration limit. This observation explains the difference between the amorphous background appearances of the two sample sets: in the case of the films obtained at 532 nm, the background is generated by the amorphous content of the films only, while in the case of the films obtained at 355 nm this superimposes on the glass substrate signal. This is particularly clear for the films deposited at λ=355 nm, 80 and 160 mTorr, where the films are thinner.

After annealing treatment at 350 ^{0}C, very well crystallised TiO_2 anatase appeared in the layers deposited at 20 mTorr and 40 mTorr (Figures 3 and 4), accompanied by a very small amount of rutile in the films prepared at λ=355 nm. The structure of the films obtained at higher pressures (80 and 160 mTorr) was not changed after heat treatment, in the sensitivity limits of the measurement, except the slight increase of the anatase peak of the film at 532 nm and 160 mTorr.

One can observe also that the titanium sub-oxides persist even in the samples with high anatase content. The amorphous phase appearance does not modify during annealing at 350 ^{0}C.

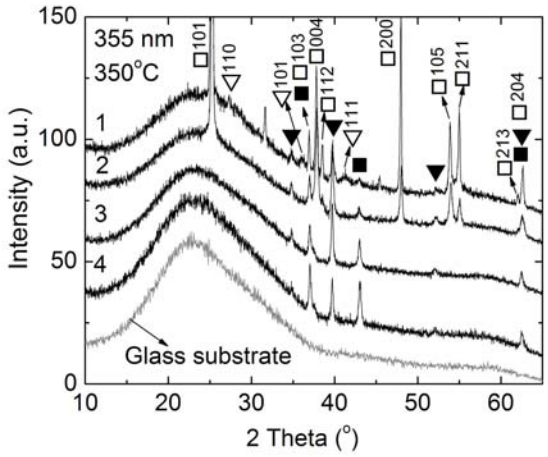

Fig. 3. XRD patterns of the films deposited at 355 nm, 350℃. Samples: 1 - 20 mTorr, 2 - 40 mTorr, 3 - 80 mTorr, 4 – 160 mTorr. Phases: □ - TiO_2 anatase, ▽ - TiO_2 rutile, ■ - TiO, ▼ - Ti_2O.

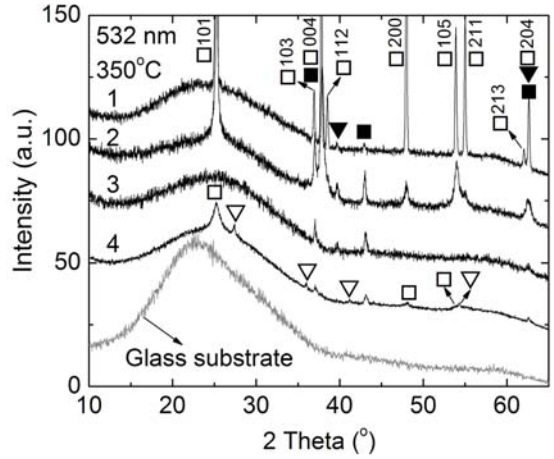

Fig. 4. XRD patterns of the films deposited at 532 nm, 350℃. Samples: 1 - 20 mTorr, 2 - 40 mTorr, 3 - 80 mTorr, 4 – 160 mTorr. Phases: □ - TiO_2 anatase, ▽ - TiO_2 rutile, ■ - TiO, ▼ - Ti_2O.

The best crystallization occurs in the layers deposited at the lowest oxygen pressure (20 mTorr), at both laser beam wavelength, and most anatase formed in the sample obtained at 20 mTorr, 532 nm.

In Fig. 5 (a-h) are presented SEM images of the films deposited with 355 nm wavelength, at 20, 40 m, 80 and 160 mTorr and annealed at 350 ^{0}C. Figures 5 (a-d) are SEM images at the film surface and (e-h) in the cross section.

One can see that at the surface, the films present droplets of different sizes and shapes. In the case of the film deposited at 20 mTorr oxygen pressure (5 a) there are more prominent droplets, some of them agglomerated. Increasing the pressure, the droplet size decreased, particularly at 160 mTorr. Also, some droplets detached from the surface, forming holes (probably during cooling process). In the case of the films deposited at 80 mTorr oxygen pressure, the structure presents incipient cracks as in figure 5 (c). At 160 mTorr oxygen pressure 5 (d), the film morphology changed, showing a noticeable porosity. The apparent porosity is a shrinkage porosity produced due to material contraction during the cooling process.

The films deposited at 20 mTorr were compact, but at increased pressure one can note individual grain formations. They can be of egg shapes or columnar.

At 80 mTorr, the film structure is columnar, the grains being tilted (5 g). In a large extent, the film porosity at 80 and 160 mTorr is a result of grain agglomerations.

The SEM images at the surface and in the cross section of the films deposited with 532 nm are shown in figures 6 (a-h). Similarly to films deposited with 355 nm laser beam on the surface there are droplets as well. At this wavelength, however the cracks appeared at lower pressure, just from 40 mTorr.

In the cross section one can note that the films deposited at 20 mTorr were compact, alike at 355 nm. Important differences are visible for films deposited at higher pressures. At 40 mTorr, the grains are columnar, the main axis being perpendicular to the substrate surface. Similarly to 355 nm, the films deposited at 80 mTorr present tilted columnar grains, but the tilt angle is randomly distributed. Also, we have to note that the grains consist of smaller spherical particles, of nanometric size.

The difference is more noticeable at 160 mTorr. In this case one can see a very porous film consisting of agglomerations of the nanometric primary particles.

Film thickness is dependent on both wavelength and oxygen pressure as is shown in Table 1.

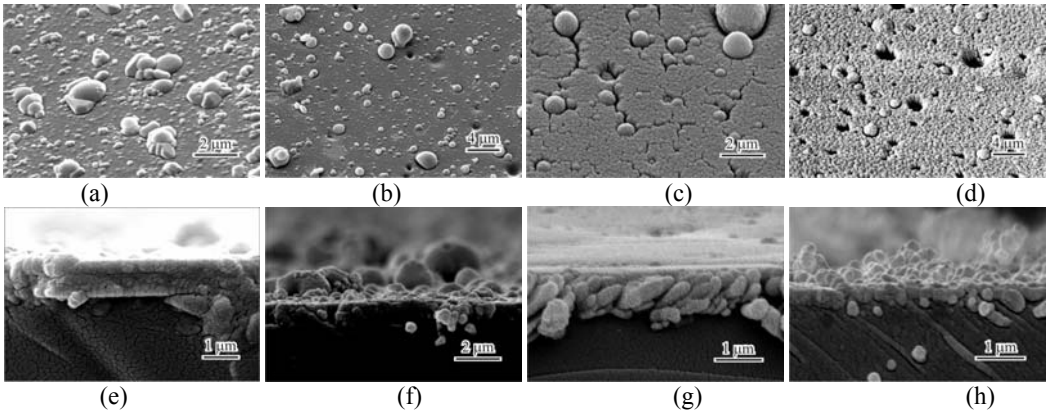

Fig. 5. SEM images of films deposited at 355 nm, annealed at 350 ^{0}C;
- at the surface: (a) 20 mTorr; (b) 40 mTorr; (c) 80 mTorr; (d) 160 mTorr;
- cross section: (e) 20 mTorr; (f) 40 mTorr; (g) 80 mTorr; (h) 160 mTorr.

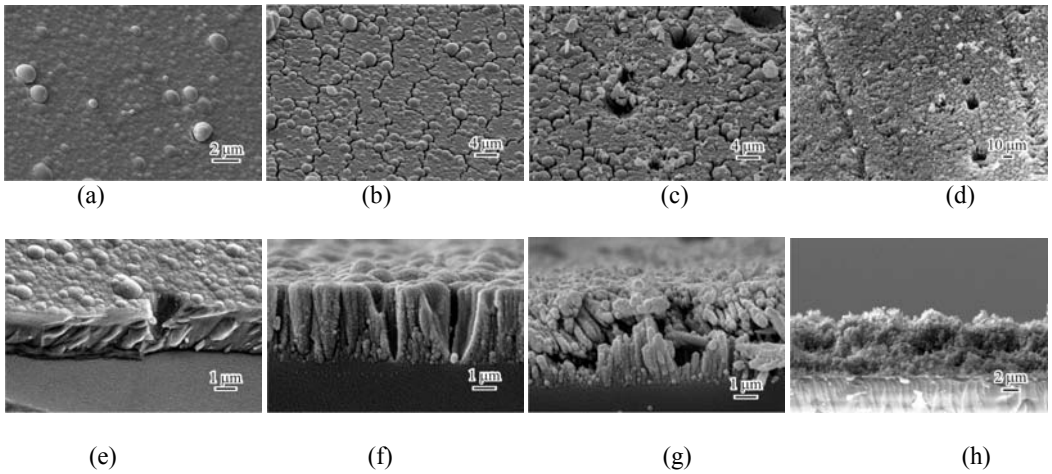

Fig. 6. SEM images of films deposited at 532 nm, annealed at 350 ^{0}C;
-at the surface:(a)20 mTorr; (b)40 mTorr; (c)80 mTorr; (d)160 mTorr;
-cross section:(e)20 mTorr; (f)40 mTorr; (g)80 mTorr; (h)160 mTorr.

Table 1. Thickness of TiO_2 films deposited on glass at 355 nm, 532 nm, RT, and annealed at 350 ^{0}C as a function of oxygen pressure and wavelength.

λ (nm)	Oxygen pressure (mTorr)	Thickness (μm)
355	20	1.00
	40	1.00
	80	0.88
	160	0.36
532	20	1.58
	40	2.92
	80	3.36
	160	5.00

First remark is that the films deposited with 355 nm, are thinner than those with 532 nm. This one can be explained by the fact that the laser radiation of 532 nm penetrating more deeply in the target, in comparison with 355 nm, the ejected particles are quantitatively more important. Another remark is that in the case of films deposited with 355 nm the thickness is decreasing if the pressure increases, while for films deposited with 532 nm the dependence is just the other way. In general at higher pressures the deposition rate is lower due to the more frequent collisions between ejected particles and gas particles (stronger particle diffusion). This aspect is predominant in the case of 355 nm.

At 532 nm there are two factors which contribute to higher deposition rates at higher pressures. The laser beam penetrating deeper into the target, the oxidation process takes place in a larger volume, and as a result the temperature is higher in a larger interaction volume. That is why the evaporation is stronger and the deposition rate higher.

4. Conclusions

Titanium oxide thin films, with thicknesses in the range 1-5 μm, were deposited on optical glass using the

pulsed laser deposition method at RT and different oxygen pressures (355 and 532 nm wavelength).

As the pressure increases from 20 mTorr to 160 mTorr, the concentration of the titanium sub-oxides with smaller oxygen content (Ti_3O and Ti_2O) decreases, while the structures enrich in TiO, regardless the laser beam wavelength.

After annealing treatment at 350 ^{0}C, very well crystallised TiO_2 anatase appeared in the layers deposited at 20 mTorr and 40 mTorr, accompanied by a very small amount of rutile (λ=355 nm). The best crystallization occurs in the layers deposited at the lowest oxygen pressure (20 mTorr), at both laser beam wavelength; most anatase formed in the sample obtained at 20 mTorr, 532 nm.

The films present droplets and cracks, depending on pressure and wavelength. At 20 mTorr the films were compact, for both wavelengths. Also, tilted or randomly distributed columnar grains were observed. The films deposited with 355 nm, were thinner than those with 532 nm. The thickness decreased if the pressure increased at 355 nm, while for films deposited with 532 nm the dependence was opposite.

Acknowledgements

This work was supported by the CNCSIS grant no.126 TD.

The author would like to thank to Dr. Mihai Vlaicu for discussions concerning XRD measurements.

References

[1] L. Zhao, M. Han, H. Lian, Thin Solid Films **516**, 3394 (2008).
[2] H. L. Ma, G. L. Guo, J. Y. Yang, Y. Guo, N.H. Ma, Nucl. Instrum. Meth. A, **264**, 61 (2007)
[3] L. Zhao, J. S. Lian, Trans. Nonferrous Metals Soc. China, **17**, 772 (2007).
[4] E. Gyoergy, A.P. del Pino, G. Shautier, A. Figueras, F. Alsina, J. Pascual, J. Appl. Phys. D, **40**, 5246 (2007).
[5] S. Murugesan, P. Kuppusami, N. Parvathavarthini, E. Mohandas, Surf. Coat. Technol., **201,** 7713 (2007)
[6] S. I. Kitazawa, Y. Choi, S. Yamamoto, T. Yamaki, Thin Solid Films, **515,** 1901 (2006).
[7] Z. W. Zhao, [13] T. Nakamura, T. Ichitsubo, E. Matsubara, A. Matsubara, N. Sato, H. Takahashi, Acta Mater., **53**, 323 (2005).
[8] T. Ohshima, S. Nakashima, T. Ueda, H. Kawasaki, Y. Suda, K. Ebihara, Thin Solid Films **506**, 106 (2006).
[9] X. S. Zhou, Y. H. Lin, J. P. Zhou, C. W. Nan, J. Phys. D-Appl. Phys., **39**,558 (2006).
[10] N. E. Stankova, P. A. Atanasov, A. O. Dikovska, I. G. Dimitrov, G. Socol, I. Mihailescu, Proc. SPIE, **5830**, 60 (2005).
[11] E. Gyorgy, G. Socol, E. Axente, I. Mihailescu, C. Ducu, S. Ciuca, Appl. Surf. Sci., **247**, 429 (2005).
[12] T. Yoshida, Y. Fukami, M. Okoshi, N. Inoue, J. Jpn. Appl. Phys. **44**, 3059 (2005).
[13] T. Nakamura, T. Ichitsubo, E. Matsubara, A. Matsubara, N. Sato, H. Takahashi, Acta Mater., **53**, 323 (2005).
[14] H. Iti, N. Takada, K. Sasaki, Appl. Phys. A-Mater., **79**, 1327 (2004).
[15] Y. Choi, S. Yamamoto, T. Umebayashi, A. Yoshikawa, Solid State Ionics, **172**, 105 (2004).
[16] S. Kitazawa, Y. Choi, S. Yamamoto, Vacuum, **74**, 637 (2004).
[17] S. Kitazawa, J. Jpn. Appl. Phys., **43**, 6335 (2004)
[18] N. Koshizaki, A. Narazaki, T. Sasaki, Appl. Surf. Sci., **197**, 624 (2002) .
[19] O. Van, R. Snyders, A. Wautelet, Appl. Surf. Sci., **254**, 974(2007).
[20] C. Sima, W. Waldhauser, J. Lackner, M. Kahn, I. Nicolae, C. Viespe, C. Grigoriu, A. Manea, J. Optoelectron. Adv. Mater., **9**, 1446 (2007).
[21] G. L. Tian, S.G. Wu, L.Y. Yang, K.Y. Shu, L.S. Qin, J.D. Shao, Chinese Phys. Lett., **24**, 2967 (2007).
[22] A.P. Caricato, S. Capone, G. Ciccarella, M. Martino, R. Rella, F. Romano, J. Taurino, T. Tunno, D. Valerini, Appl. Surf. Sci., **253**, 7937 (2007).
[23] A.P. Caricato, M.G. Manera, M. Martino, R. Rella, F. Romano, J. Spadavecchia, T. Tunno, D. Valerini, Appl. Surf. Sci., **253**, 6471 (2007).
[24] A. Niilisk, M. Moppel, M. Pars, I. Sildos, T. Jantson, T. Avarmaa, R. Jaaniso, J. Aarik, Centr. Eur. J. Phys., **4**, 105 (2006).

*Corresponding author: simac@ifin.nipne.ro